42nd AIAA/ASME/SAE/ASEE Joint Propulsion Conference & Exhibit
9 - 12 July 2006, Sacramento, California

AIAA 2006-4818

Multi-Axis Plasma Profiling System for Characterization of Plasma Thruster Plumes

Casey C. Farnell,[1] Molly M. Schmidt,[2] Robert L. Millot,[2] Dustin J.Warner,[2]
Kyle Siler-Evans,[2] and John D. Williams[3]
Colorado State University, Fort Collins, CO 80523

Abstract

A three-degree of freedom, actuator-based system is described for positioning an ion current density probe within the near field region of plasma and ion thrusters. This system improves upon existing beam profiling systems which usually characterize plasma and ion beams by sweeping a Faraday probe through a single motion at a fixed axial (or radial) distance downstream of a device under test. Fully automated computer control is used for positioning the probe, data collection and analysis, and to interface via communication ports to power supply and vacuum chamber control systems. The three-axis probe actuator system is capable of obtaining improved ion beam data critical for calculating plume uniformity, beam symmetry, total energetic particle flux through a given plane, beam divergence, beam centroid, thrust vector direction, etc. The high resolution data collected with this tool are planned for use in validating numerical simulations of the plasma plume properties of ion and plasma thrusters. Experimental results are presented that demonstrate the capabilies of the beam profiling system on a Veeco Instruments 5-cm DC ion source. A total of 15 operating conditions were characterized by taking planar (x-y) scans of the ion beam at axial (z) distances ranging from 12.5 to 32.5 cm. Beam ion energies ranging from 200 to 1000 eV were evaluated at beam currents from 30 to 90 mA. The measurements were analyzed to calculate the effects of beam ion energy, beam current, and charge exchange and ion scattering on the beam shape and attenuation. The attenuation data were reduced to determine estimates of charge exchange cross section, and good agreement was observed with values available in the literature.

1.0 Introduction

Ion current density measurements can be used to calculate ion and plasma source parameters such as beam uniformity, beam symmetry, total energetic particle flux through a given plane, beam divergence, beam centroid, thrust vector direction, etc.[1,2] In an ideal beam, ions would exit uniformly across the face of an ion or plasma source, however, due to imperfect plasma production and extraction as well as processes that occur within the beam plasma such as charge exchange and scattering, a real ion beam displays complexly varying current density behavior as a function of position. Current density, along with ion energy, plays a major role in determining the effects of an ion beam when (1) it is directed onto the surface of a material and (2) in applications requiring fine control of thrust. Because of this, it is useful to measure and understand how current density varies at locations downstream of an ion or plasma source.

[1] Graduate Research Assistant, Mechanical Engineering, 1320 Campus Delivery, AIAA Student Member
[2] Undergraduate Research Assistant, Mechanical Engineering, 1320 Campus Delivery
[3] Assistant Professor, Mechanical Engineering, 1320 Campus Delivery, AIAA Senior Member

These measurements are important for validating numerical simulations that are now being used to estimate the plume properties of ion and plasma thrusters intended for use on spacecraft.

This paper is broken down into two sections. In the first section, we describe the apparatus used to perform current density measurements in the volume downstream of ion and plasma thrusters. This section includes information on the (1) design of the test apparatus, (2) ion current density measurement technique, (3) cooling and thermal management, (4) electrical setup, and (5) operator interface to the computer control system. In the second section, we describe measurements made on a Veeco Instruments 5-cm DC, internally-mounted, water-cooled ion source. The ion source is capable of operating at beam voltages ranging from 50 to 2000 V and beam currents of 25 to 200 mA. A total of 15 operating conditions were characterized by taking planar (x-y) scans of the ion beam at axial (z) distances ranging from 12.5 to 32.5 cm from the ion source. Beam ion energies ranging from 200 to 1000 eV were evaluated at beam currents from 30 to 90 mA. Because measurements were made at different axial distances, it was possible to determine the mean free path due to charge exchange and scattering collisions through measurement of how the total integrated beam current varied as a function of axial distance. Charge exchange cross sections were calculated from the mean free path measurements and estimates of the neutral density within the ion beam. Good agreement was observed between the calculated charge exchange cross sections and values available in the literature, and this agreement is used to suggest that the current density measurement apparatus is performing correctly.

2.0 The Multi-Axis Plasma Profiling System (MAPPS)

The multi-axis plasma profiling system was built for the purpose of making measurements of ion current density in the volume downstream of ion and plasma devices. The overall goal was to fully characterize a source in a minimal amount of time and to eliminate the need for an operator to monitor the system during testing. A secondary goal was to make the system reliable enough to perform continuous measurements of a particular ion or plasma source at a dozen or more operating conditions in about 17 hrs. In this way, the resulting data would be available for analysis on the following day while a new device was installed for subsequent characterization.

A photograph of the MAPPS apparatus is shown in Fig. 1 along with an exploded solid model showing the main components of the system. Figure 2 shows an image of how the system was mounted in a cylindrical vacuum chamber. Much of the mechanical design of the MAPPS was based upon the geometry of the cylindrical vacuum chamber, which was 63 cm in diameter and 81 cm tall. As shown in Fig. 2, the ion source is mounted on the top flange of the vacuum tank and pointed down toward the bottom of the chamber. Because of the chamber geometry, the MAPPS system was designed to mount in the bottom of the chamber with the measurement probe pointed up toward the ion source. An orificed Faraday probe described in Section 2.1 was used to make current density measurements because of its compact size and relative ease of use.

In order to position the Faraday probe within the three dimensional r-θ-z (or x-y-z) space, three high-resolution stepper motors were used. The theta stage stepper motor is attached to a 20:1 gearbox which rotates the system in the theta direction. The radial stage motor sits on top of the theta stage and attaches to a linear drive screw which enables movement in the radial direction. Similarly, axial movements are accomplished with the axial linear stage, which is attached on top of the radial stage. Figure 2 also contains an image of the system viewed from the top as seen by the ion source. Limit switches were placed on each of the movement stages

for zeroing purposes and also to prevent the stages from being moved too far in any of the travel directions. The Faraday probe is mounted on a rod extending from the axial stage and angled slightly outward to achieve the maximum amount of probe scan area within the cylindrical volume of the vacuum chamber. To the largest extent possible, the components of the system were kept below the level of the Faraday probe to minimize effects on the ion beam.

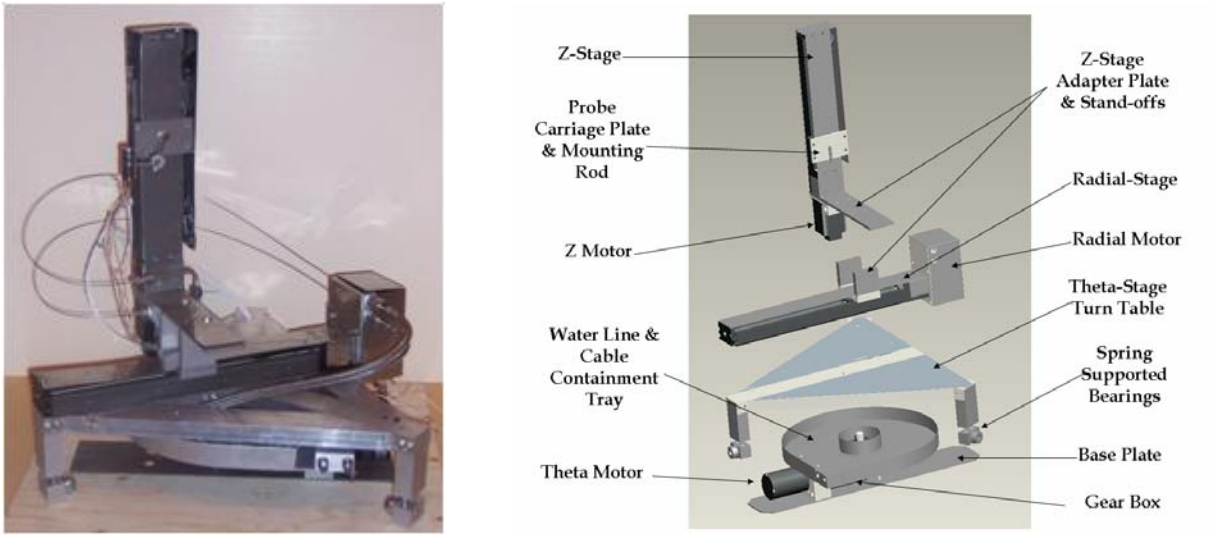

Figure 1 *Mechanical design of the system. Three stepper motors are used to position a Faraday probe in a three dimensional space.*

2.1 Ion Beam Current Measurement

A Faraday probe, shown in Fig. 3, was used to measure the ion beam current density at a given location within the ion beam.[3] Ions from the beam enter the probe through the body aperture and strike the collector disk. The current is measured by reading the voltage across a resistor that is placed in the electrical lead between the collector disk and ground. The current density is then calculated using:

$$j_B = \frac{V \cdot 1000}{R \cdot A_{aperture}} \quad (\text{mA/cm}^2) \qquad (1)$$

Where V is the voltage across the resistor (Volts), R is the value of the resistor (Ohms) and $A_{aperture}$ is the area of the opening (cm^2). The aperture sets a specific collection area since the collector disk is made to be larger than the aperture opening. The collector plate is biased positive (30V) of ground in order to repel any low energy charge exchange ions that exist within the vacuum tank. The probe cap and body are biased negative (-30V) to repel beam plasma electrons from reaching the collector plate. In addition, the combination of the negative bias on the body and the positive bias on the collector disk serves to eliminate secondary (or Auger) electron emission from the collector. In this bias scheme, all secondary electrons that are generated from ions striking the collector disk will return back to the collector due to the adverse potential gradient created between the body and the collector disk.

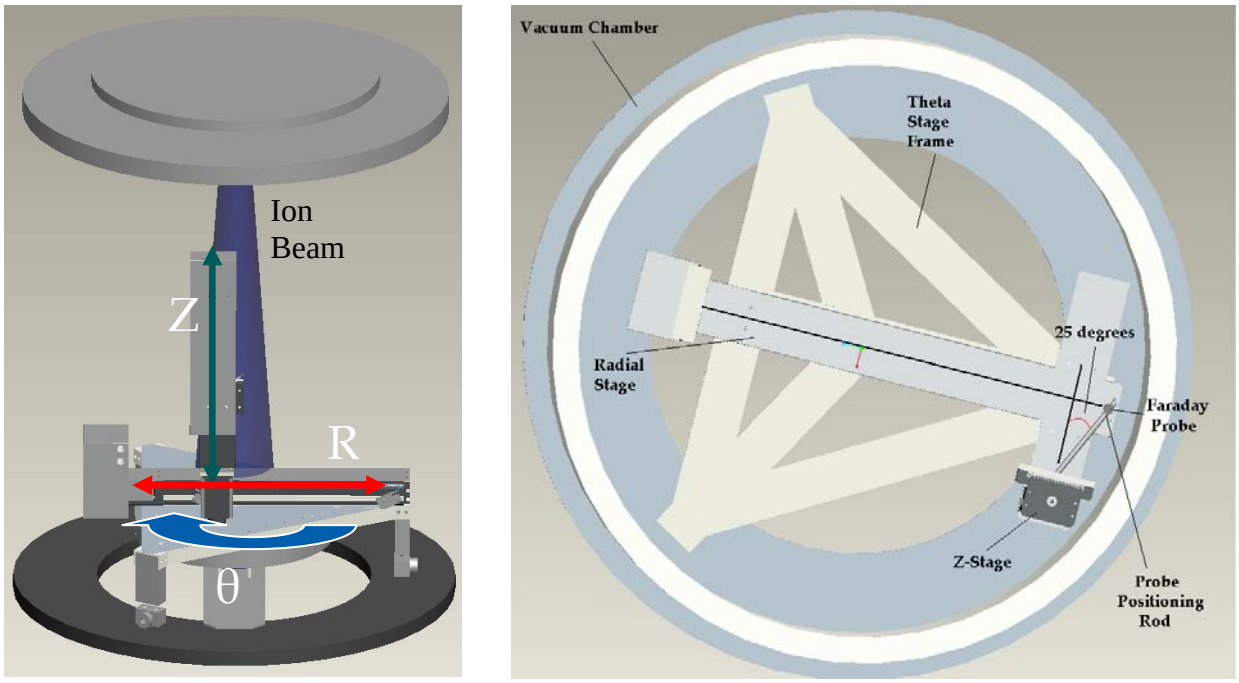

Figure 2 *Layout of the system within the vacuum tank. The ion source is mounted on the top flange and pointed down. Using a combination of radial, theta, and axial moves, a Faraday probe is used to map the current density of ion and plasma sources in three dimensions.*

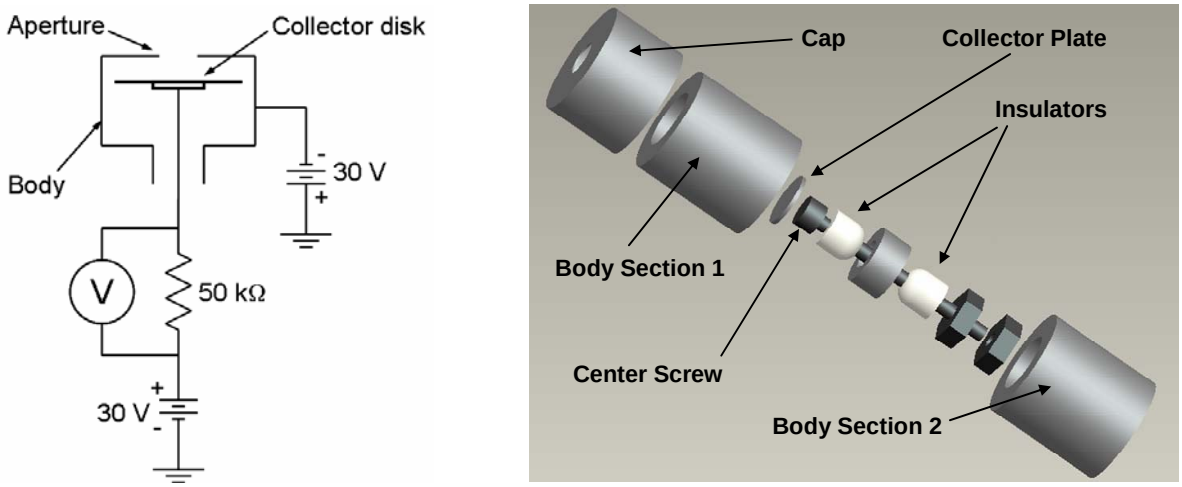

Figure 3 *Electrical schematic and model of the Faraday probe used to measure the ion current.*

2.2 MAPPS Cooling and Thermal Management

Due to the geometry of the vacuum tank and the position of the ion source, the Faraday probe and the entire actuation system is partially exposed to the ion and plasma plumes. As much as possible, the motors and electrical limit switches were located at large radial positions to remain outside of the highest intensity plume regions. All of the system components were clad with stainless steel radiation shields to (1) prevent direct ion impingement and subsequent sputtering of components and (2) reduce heat loading caused by ion and plasma plume impingement. In addition, a water cooling system was designed for the three stepper motors.

Figure 4 illustrates the water cooling system. Water flows through a series of aluminum cooling blocks that are attached to each of the motors. This arrangement was chosen based on the geometry of the actuation system. Flexible water lines are used for cooling the radial and axial motors because the motors move when the system is taking measurements. The cooling lines between the theta and radial motors are allowed to wind and unwind as the system is moving in the theta direction. Small diameter stainless steel water lines are used between the radial and axial motors so that the tubing can flex while the system is performing radial movements.

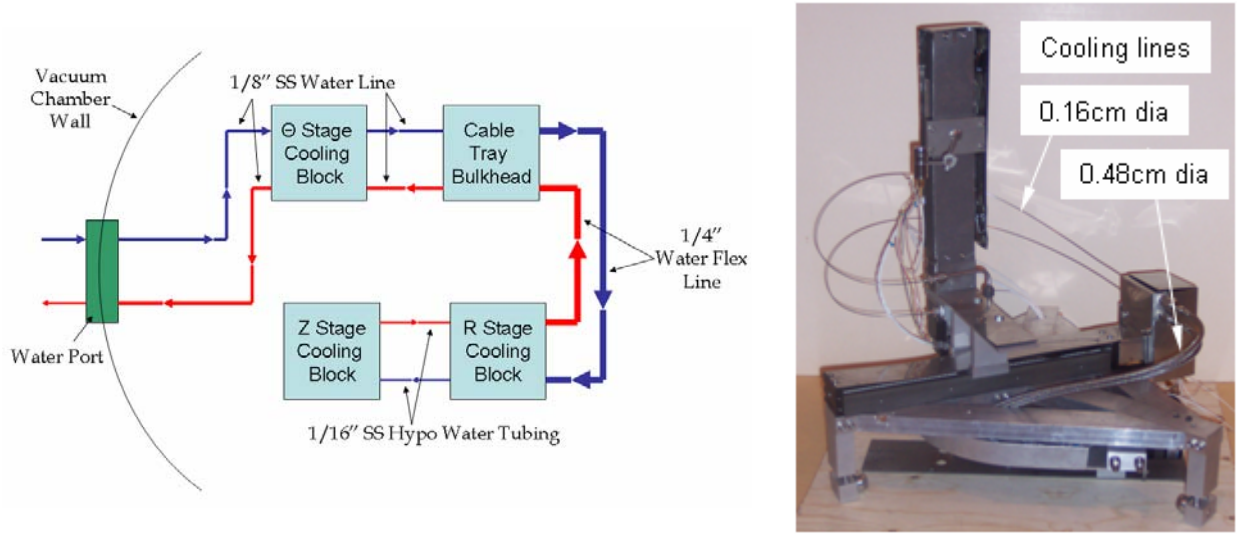

Figure 4 *Diagram and picture of the stepper motor cooling system. Water flows through aluminum cooling blocks that are directly attached to the stepper motors to keep the motors from overheating.*

2.3 Electrical Setup

The MAPPS is controlled through the use of a computer. Figure 5 shows the setup for the control of the movements as well as how the Faraday probe measurements were made. All motion control is achieved via a serial interface between the computer and a Trio motion controller. The movement calculations are done in a computer program and the actual move commands are sent to the Trio controller. Once the probe move has been completed, a computer-based data acquisition program records the ion current density. Then, the next set of movement commands are sent to the motor controller and another measurement is made. The process is repeated until all measurements have been completed for the requested scan sequence.

2.4 Operator Interface

Figure 6 shows a screenshot of the overall MAPPS computer program. Here the user can access various subroutines to setup and initiate data collection operations. The mapping choices consist of 1D radial scans across the diameter of the beam, or 2D (x-y planar) and 3D (x-y-z) scans. For the 2D and 3D beam scans, the MAPPS uses a Cartesian coordinate system to position the probe. The computer program calculates the proper axial, radial, and theta stage movements to reach the specified x-y-z position. The use of a Cartesian coordinate system made more sense in terms of simplifying the post test data processing and analysis.

Once the program is started, two interlock features of the system are enabled. The first involves monitoring the exit water flow that cools the three stepper motors. The second involves

monitoring the pressure within the vacuum tank. If the water flow falls below a preset value or if the pressure in the tank goes above a preset value, the computer program will turn the ion source off, stop taking measurements, and shut off the water flow. These interlocks were implemented in case of (1) a water cooling blockage or shutoff or (2) failure of an in-vacuum water line, development of a severe vacuum leak, or pump failure. Low water flow could cause the motors to overheat and a water leak or vacuum system failure could damage the ion or plasma source being tested.

Another feature of MAPPS is its ability to communicate and control the source operating condition. This was done though a serial communications interface to the power supply that enabled the system to fully characterize an ion or plasma device while minimizing the need for an operator to continually monitor the system. With this feature, the operator can input a set of ion source operating conditions at the beginning of the testing period, and then the system performs the prescribed sequence of probe measurements at each of the prescribed source conditions.

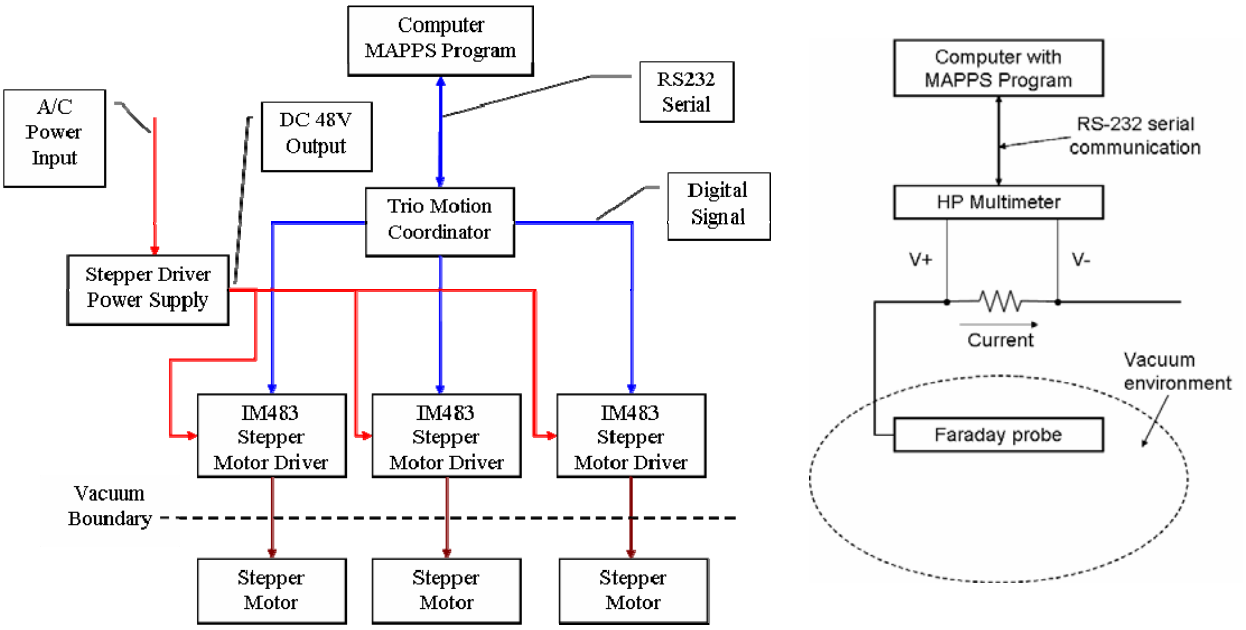

Figure 5 *Simple diagrams showing the electrical and measurement setup. The computer program communicates movement commands to the Trio motor controller and requests current density measurements from an HP multimeter.*

3.0 Testing Procedure and Results

The MAPPS was used to characterize a Veeco Instruments 5-cm DC ion source. To characterize the source, 15 operating conditions were chosen that comprised 5 beam voltages of 200, 400, 600, 800, and 1000V and 3 beam currents of 30, 60, and 90 mA. The ion source was controlled by a computer program through RS-232 serial communication with a fully integrated Veeco MPS 3000 power supply that is equipped with fault detection. At each of these operating conditions, probe measurements in x-y planes were taken at 5 axial (z) distances from the source. Each source condition took about 1.1 hr to profile for a total test time of ~17 hr.

Figure 7 shows a contour and surface plot of ion current density measurements taken at one axial location. The x-y plane was mapped by taking 21 x 21 probe measurements (i.e., 441 measurements). Because the beam shape varied at each source condition and axial distance from the source, a different planar area was scanned to measure an appropriate amount of the beam. This variable planar scan area ensured that enough measurements were taken where the current density data was most valued (usually in the center of the beam where the current density was the greatest and varied the most).

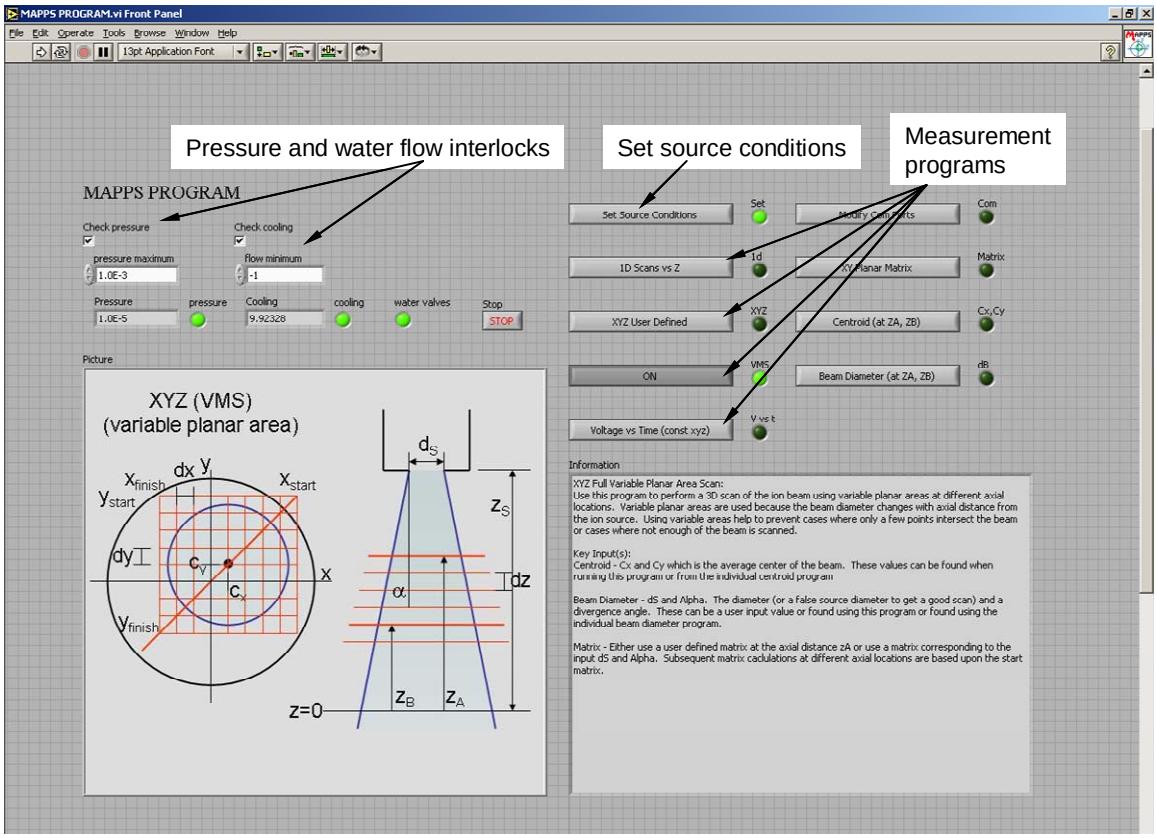

Figure 6 *Computer user interface. The program can monitor the pressure in the vacuum chamber and cooling flow to the motors while measurements are being taken.*

As explained above, there were three main variables involved during the characterization of the 5-cm ion source; beam voltage, beam current, and axial distance from the source. As expected, changing any of these three values caused the current density reading to change. Figure 8 illustrates how the ion beam shape changes when the axial distance from the ion source was varied. For each of the 15 operating conditions, x-y planes were mapped at 5 axial distances of 12.5, 17.5, 22.5, 27.5, and 32.5 cm from the grid set. Also as expected, the current density peaked in the center of the ion beam and was highest when profiling at the closest axial distance (see Fig. 8a). Looking at the progression of current density plots, the beam grew wider (and flatter) at planes farther downstream from the source. The divergence of the beam, combined with lesser effects of ion scattering and charge exchange in the vacuum tank, caused the beam shape and current density to vary.

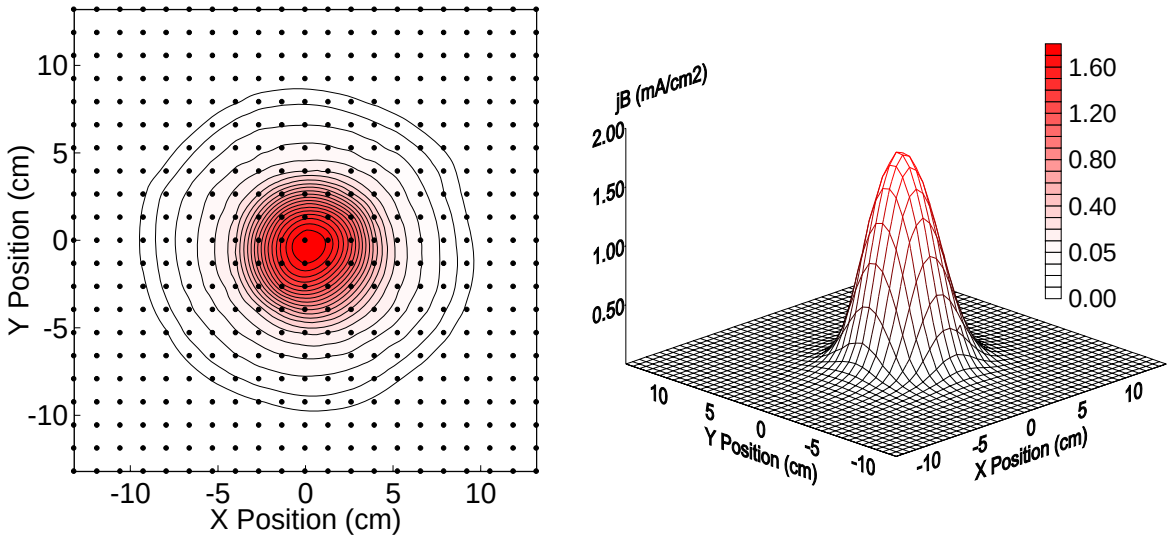

Figure 7 *Example planar (x-y) contour and surface plots showing where the probe measurements were taken. An array of 21x21 points for each axial location downstream of the ion source were measured. (J_B = 90 mA, V_B = 800 V, z = 27.5 cm).*

Ions are extracted from an ion source depending on the grid set geometry and applied voltages.[4] The effect of beam or net voltage can be seen in Fig. 9 over a range from 200 to 1000 V. It is noted that the same total voltage of 1100 V was applied between the screen and accelerator electrodes for all of the tests described herein. As expected, the ion beam was more collimated as the beam voltage was increased from 200 V (Fig. 9a) to 1000 V (Fig. 9e) as the R value ($R=V_n/V_t$) was increased from 0.18 to 0.91. While the shape of the beam changed, integration of all of the 5 current density data sets resulted in a beam current near 30 mA, which was approximately equal to the beam current measurement taken from the power supply system.

Similar to applied voltages, the prevailing beam current also affects the plume characteristics due to (1) space charge effects and (2) sheath shape changes that occur nearby apertures in the screen electrode. As mentioned above, three beam currents were tested (30, 60, and 90 mA), and Fig. 10 shows plots of the current density variation for these beam currents at a beam voltage of 600 V and an axial distance of 22.5 cm. For the 5 cm ion source at this voltage setting, the beam shape diameter was largest at the 30 mA beam current (see the gray contour data shown in Fig. 10d). The beam shape narrowed (blue and yellow) at the 60 and 90 mA beam current settings.

Finally, the current density measurements are affected (attenuated) by particle interactions that occur in the volume between the ion source and the Faraday probe. Both charge exchange reactions and ion scattering cause lower than expected current density measurements.[3,5] The magnitude of this attenuation is determined by the distance to the probe, the number density of particles participating in the collision processes, and the combined cross section of scattering and charge exchange reactions. Ion scattering occurs when a fast moving beam ion collides with a slow moving ion or neutral and its trajectory is altered so that the ion can no longer be detected by the axially oriented Faraday probe. Charge exchange is a process whereby an electron from a slow moving neutral is transferred to a fast moving beam ion. When this occurs, the fast moving ion becomes a fast moving neutral and the slow moving neutral becomes a slow moving ion. The Faraday probe design and voltage bias scheme used in MAPPS only allows measurement of fast moving ions (>30 eV). Figure 11 shows a plot of the

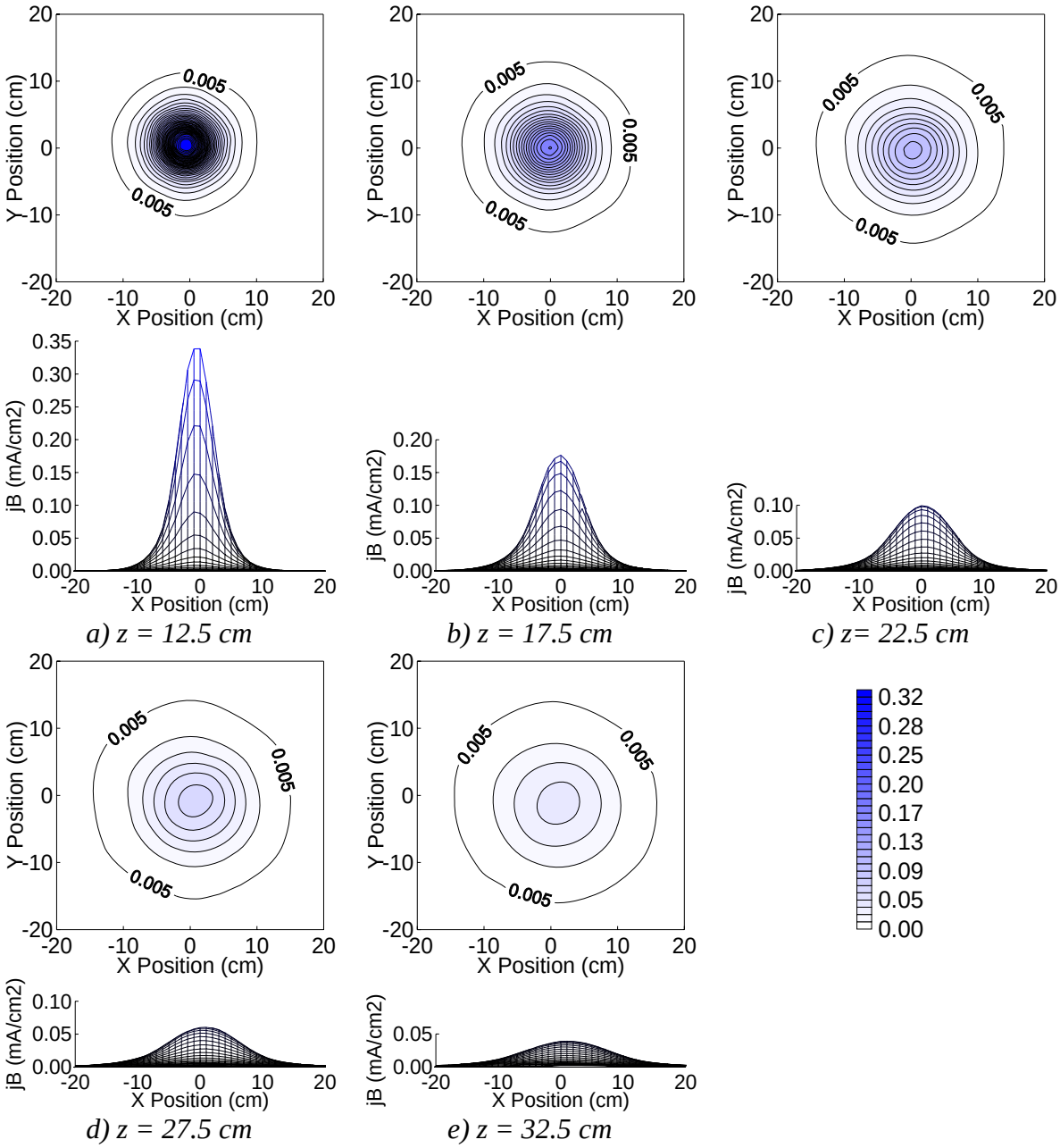

Figure 8 *Contour and surface plots showing effect of axial distance (z) from the ion source. The beam voltage (V_B = 200 V) and beam current (J_B = 30 mA) were held constant.*

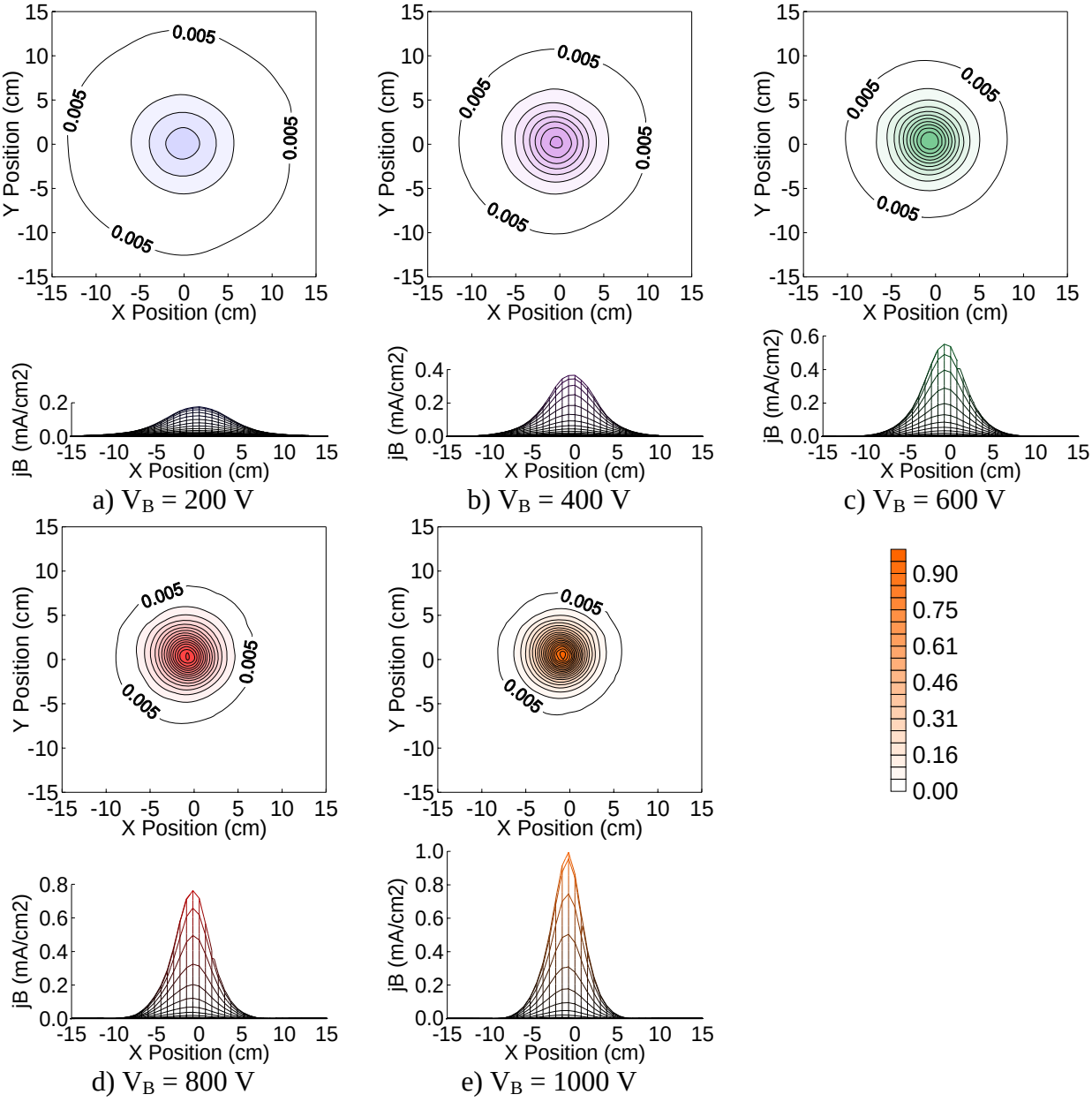

Figure 9 *Effect of beam voltage (i.e., ion energy) on current density variation. Note that the beam current (J_B = 30 mA) and axial location (z = 17.5 cm) were held constant and that integration of the current density contours resulted in beam current values close to the measured beam current of 30 mA.*

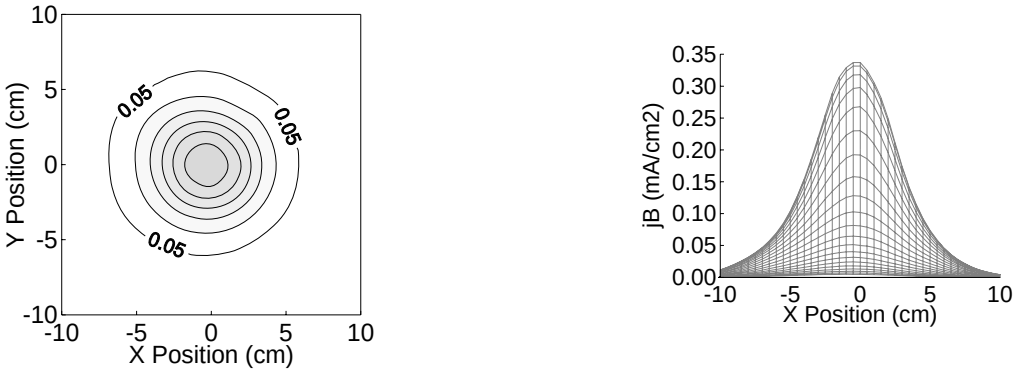

a) J_B = 30 mA

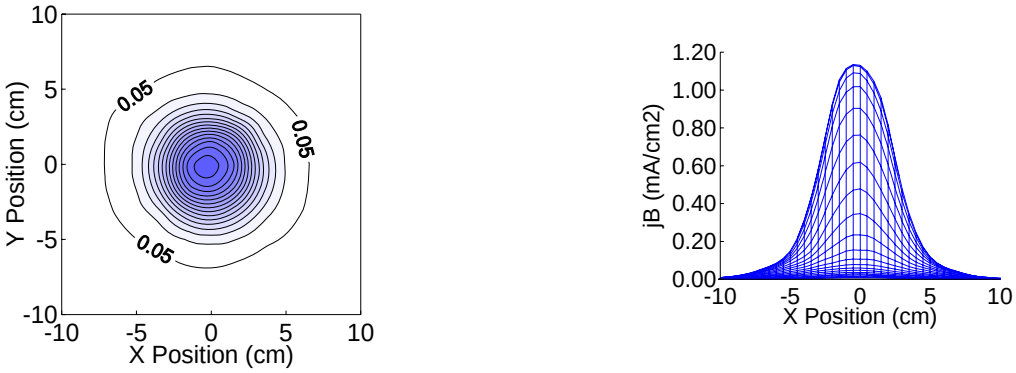

b) J_B = 60 mA

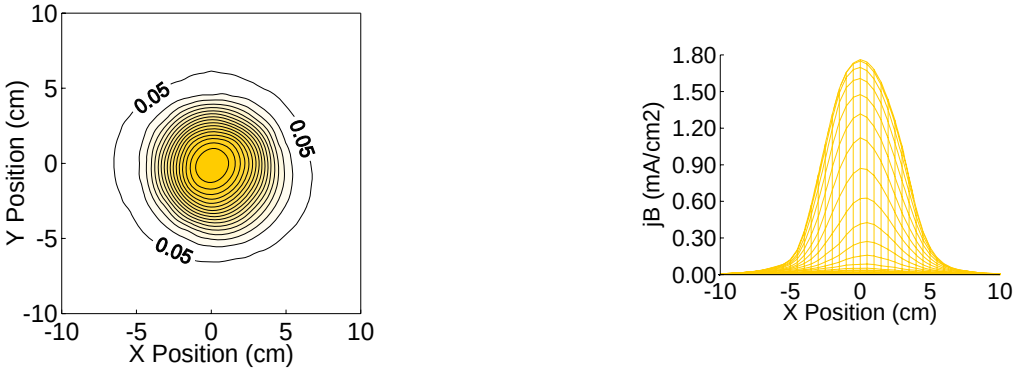

c) J_B = 90 mA

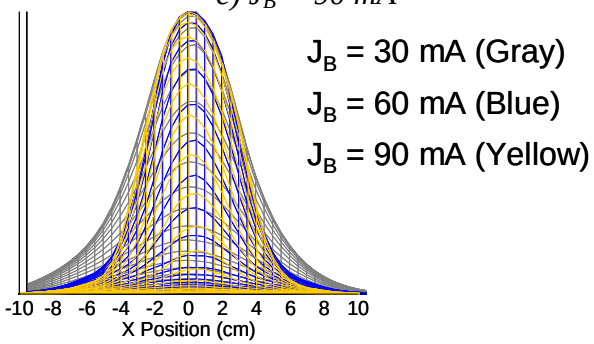

d) Normalized plots overlaid to illustrate beam focusing.

Figure 10 *Effect of varying the beam current at V_B = 600 V and z = 22.5 cm.*

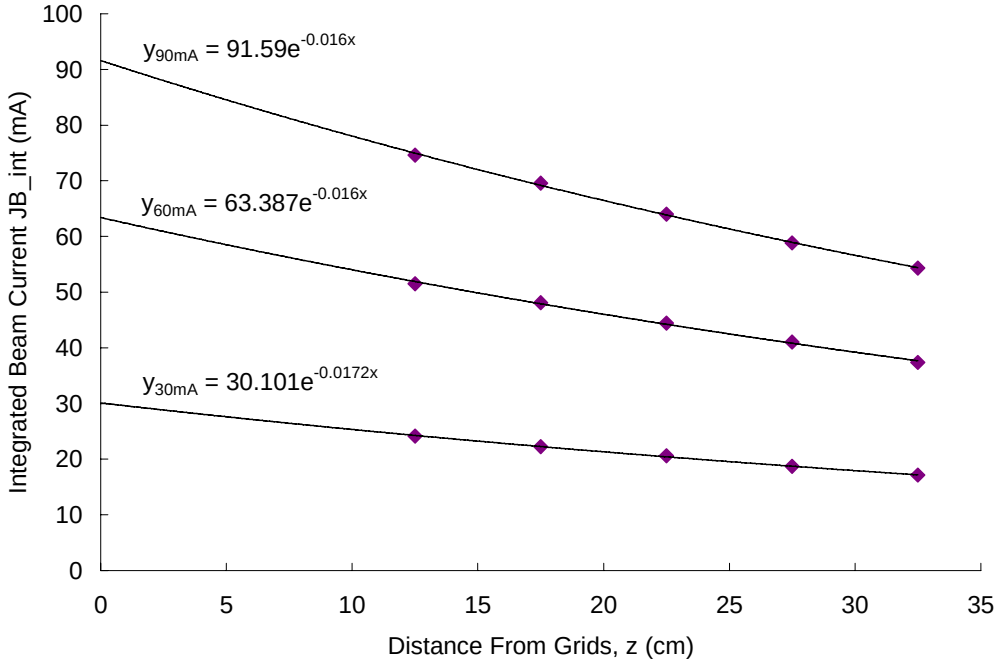

Figure 11 *Numerically integrated beam currents at a beam energy of 400 V. Each curve corresponds to a power supply indicated beam current of 30, 60, or 90 mA. Ion scattering and charge exchange collisions cause an exponential decrease in the integrated beam current with axial distance.*

integrated beam current at each axial location downstream from the grids at an energy of 400 V. The exponential trendline curve fit shown in Fig. 11 was assumed to be of the form:

$$J_B(z) = J_{B0} e^{\frac{-z}{\lambda_{CEX+SC}}} \text{ (mA)} \quad . \quad (2)$$

In Eq. (2), $J_B(z)$ represents the measured beam current (mA) passing through the x-y plane located at z, J_{B0} the actual beam current originating from the ion source (mA), λ_{CEX+SC} the overall mean free path of the ions due to charge exchange and scattering collisions (cm), and z the distance from the source (cm). As can be seen, the extrapolation of the trendline back to z = 0 yields a value that is in good agreement with the beam current measured by the power supply system.

The mean free path measurement made from the curve fits shown in Fig. 11 can be converted into a combined cross section value using the equation:

$$\sigma_{CEX+SC} = \frac{1}{n \cdot \lambda_{CEX+SC}} \quad (\text{m}^2) \quad . \quad (3)$$

In Eq. (3) σ_{CEX+SC} represents the combined cross section for argon ions (m^2) and *n* the neutral density of particles in the tank (m^{-3}). Figure 12 shows comparisons of the charge exchange cross sections calculated from attenuation data like those shown in Fig. 11. Note that the data are

plotted as the square root of the cross section versus ion energy. Throughout the tests described herein, the flow rate was held constant at 1.2 sccm Ar and the pressure in the vacuum chamber in the region between the ion source and the measurement apparatus was estimated to be 1.3×10^{-4} Torr. The actual measured pressure was 8.8×10^{-5} Torr, but the ion gauge was located below the measurement apparatus and immediately above the cryopump port. Also note that only results for the 30 and 60 mA beam current conditions are shown in Fig. 12. The 90 mA beam current data were not used because the source was operated at an uncorrected propellant utilization close to unity, and it is likely that a significant fraction of the beam (~30%) was made up of doubly charged argon ions that would introduce errors into the charge exchange cross section calculations. The charge exchange cross sections at the 30 and 60 mA beam conditions were found using the equations:

$$\sigma_{CEX} = \sigma_{CEX+SC} - \sigma_{SC} \quad (\mathrm{m}^2) \tag{4}$$

and

$$\sigma_{SC} = \pi \cdot (2 \cdot r_{AR})^2 \quad (\mathrm{m}^2) \quad . \tag{5}$$

In Eqs. (4) and (5), r_{AR} represents the atomic radius of argon ($0.88*10^{-20}$ m) and σ_{SC} represents the scattering cross section ($\sigma_{SC}=9.73*10^{-20}$ m^2) assumed to be constant over the ion energy range that was investigated. Figure 12 compares these data to the calculations of Rapp and Francis and more recent data of Sakabe and Izawa.[6,7] The present study indicates values that are within +36% and -16% of Sakabe and Izawa. This level of agreement is considered to be acceptable due to the uncertainties in neutral pressure ($\pm$50%) and temperature ($\pm$10%) in the present experiment.

4.0 Conclusions

A system was built that is capable of positioning a Faraday probe throughout the three-dimensional volume of ion and plasma plumes for the purpose of making current density measurements. A demonstration of the system was performed where a predetermined sequence of current density measurements was made at 15 operating conditions of a Veeco Instruments 5-cm diameter ion source while simultaneously monitoring the vacuum tank pressure and motor cooling water flow for leaks or other problems. The automatic controls included changing the power supply beam voltage and beam current between 3-D scans so that the ion source could be characterized without operator assistance. Results were presented to show the capability of the system by examining how the current density profile changed when the beam voltage, beam current, or axial probe distance was varied. For the grid set tested, the shape of the beam narrowed and the peak current density increased when the beam voltage was increased, the beam current was increased, or the probe was moved closer to the ion source. The current density measurements with axial position were used to estimate cross section values. The measured argon charge exchange cross sections were in good agreement with values available from the literature, and the cross sections were observed to decrease as the ion energy was increased, which is also in agreement with trends predicted in the literature.

Acknowledgments

The authors would like to thank Veeco-Fort Collins for their financial support of the project as well as providing test equipment, an ion source, and power supply system.

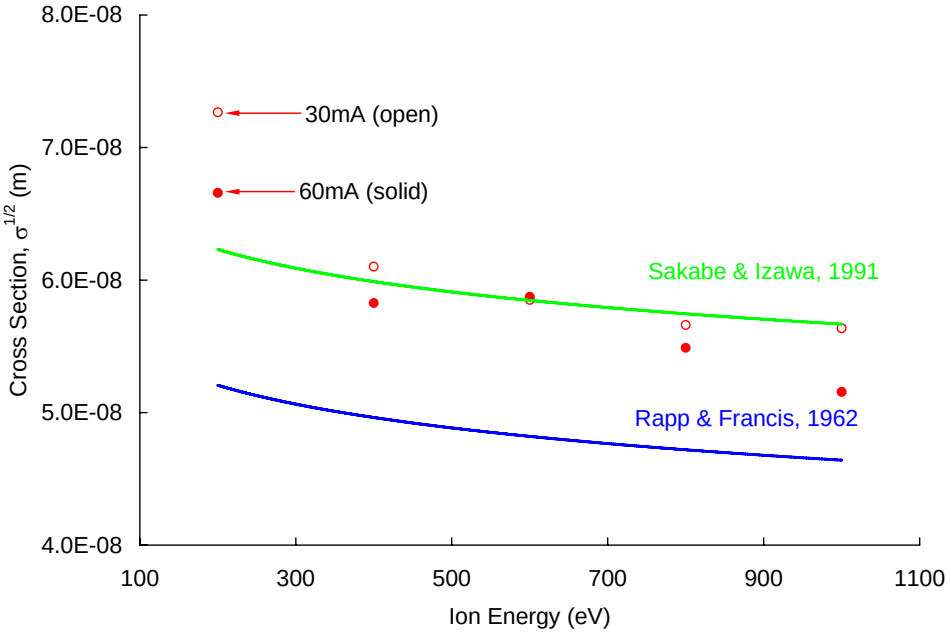

Figure 12 *Charge exchange cross section as a function of ion energy. The charge exchange cross section was estimated by subtracting an assumed scattering cross section from the combined cross section data calculated from attenuation measurements like those shown in Fig. 11. Errors of +36% to -16% were observed relative to Sakabe & Izawa, 1991.*

References

[1] Snyder, A., Kamhawi, H., Patterson, M., and Britton, M., "Single-String Integration Test Measurements of the NEXT Ion Engine Plume," AIAA-2004-3790, 40th Joint Propulsion Conference, Fort Lauderdale, FL, 2004.

[2] Haag, T., "Translation Optics for 30 cm Ion Engine Thrust Vector Control," IEPC-01-116, 27th International Electric Propulsion Conference, Pasadena, CA, 2001.

[3] Hofer, R.R., Walker, M.L.R., and Gallimore, A.D., "A Comparison of Nude and Collimated Faraday Probes for Use with Hall Thrusters," IEPC-01-020, 27th International Electric Propulsion Conference, Pasadena, CA, 2001.

[4] Rawlin, V.K., Williams, G.J., Pinero, L.R., and Roman, R.F., "Status of Ion Engine Development for High Power, High Specific Impulse Missions," IEPC-01-096, 27th International Electric Propulsion Conference, Pasadena, CA, 2001.

[5] Reynolds, T.W., and Richley, E.A., "Contamination of Spacecraft Surfaces Downstream of a Kaufman Thruster," NASA Technical Note D-7038, Lewis Research Center, Cleveland, OH, Jan. 1971.

[6] Rapp, D., and Francis, W.E., "Charge Exchange between Gaseous Ions and Atoms," Journal of Chemical Physics, Vol. 37, No. 11, Dec. 1, 1962.

[7] Sakabe, S., and Izawa, Y., "Cross Sections for Resonant Charge Transfer Between Atoms and Their Positive Ions: Collision Velocity < 1 a.u.," Atomic Data and Nuclear Data Tables, Volume 49, No. 2, p. 257-314, 1991.